

Research Article

Influences of Ultrafine Slag Slurry Prepared by Wet Ball Milling on the Properties of Concrete

Yubo Li ¹, Shaobin Dai,¹ Xingyang He ², and Ying Su²

¹Wuhan University of Technology, Wuhan 430070, China

²Hubei University of Technology, Wuhan 430070, China

Correspondence should be addressed to Xingyang He; lunwenhe2017@sina.com

Received 27 December 2017; Accepted 23 April 2018; Published 4 June 2018

Academic Editor: Sverak Tomas

Copyright © 2018 Yubo Li et al. This is an open access article distributed under the Creative Commons Attribution License, which permits unrestricted use, distribution, and reproduction in any medium, provided the original work is properly cited.

The application of ultrafine ground-granulated blast-furnace slag (GGBFS) in concrete becomes widely used for high performance and environmental sustainability. The form of ultrafine slag (UFS) used in concrete is powder for convenience of transport and store. Drying-grinding-drying processes are needed before the application for wet emission. This paper aims at exploring the performances of concrete blended with GGBFS in form of slurry. The ultrafine slag slurry (UFSS) was obtained by the process of grinding the original slag in a wet ball mill, which was mixed in concrete directly. The durations of grinding were 20 min, 40 min, and 60 min which were used to replace Portland cement with different percentages, namely, 20, 35, and 50, and were designed to compare cement with original slag concrete. The workability was investigated in terms of fluidity. Microstructure and pore structure were evaluated by X-ray diffraction (XRD), scanning electron microscopy (SEM), and mercury intrusion porosimetry (MIP). The fluidity of concrete mixed with UFSS is deteriorated slightly. The microstructure and early strength were obviously improved with the grind duration extended.

1. Introduction

Cement, the main cementitious material used in the concrete, is the base material of construction. Cement manufacture is a highly energy-intensive process. The total energy consumption of the global cement industry is estimated at 2% of global primary energy use, which accounts for approximately 7% of all global carbon dioxide emissions [1, 2]. The development of ecofriendly concrete in the construction industry is gaining deep concern and intensive research worldwide.

Ground-granulated blast-furnace slag (GGBFS) is a by-product of steel making [3]. GGBFS has been found to exhibit excellent cementitious properties when it was finely powdered [4]. The use of GGBFS as supplementary cementitious material not only reduces the usage of cement [5] but also improves the porosity performance of OPC concrete [6]. In addition, GGBFS is one of the major precursor materials used in the production of alkali-activated materials (AAMs) [7]. As a kind of alternative cementitious material, GGBFS shows comparable mechanical performance to

blended slag cement and similar or even lower global warming potential compared with the best available concrete technology [8]. The reactivity of GGBFS is considered an important parameter to assess the effectiveness of GGBFS in concrete composites, which varies greatly with the source of slag, types of raw material used, methods of cooling, and the duration of milling [9]. Pal et al. [10] investigated the relationship between the hydraulic index (HI) of slag and the influencing factors of slag, including glass content, fineness, and chemical composition. Zhao et al. [11] studied the particle characteristics and hydration activity of GGBFS containing industrial crude glycerol-based milling aids. The result indicated that means and milling aids strongly affect the activity of GGBFS.

Wet milling is a method of producing powder slurry by milling materials with mediums together, with advantages of uniformity, high milling efficiency, and small noise contrast with dry milling. It is widely used in cement and ceramics industries [12] and rarely in the field of slag powder. Nowadays, the main milling methods of slag are dry milling processes and need to go through drying-milling-drying

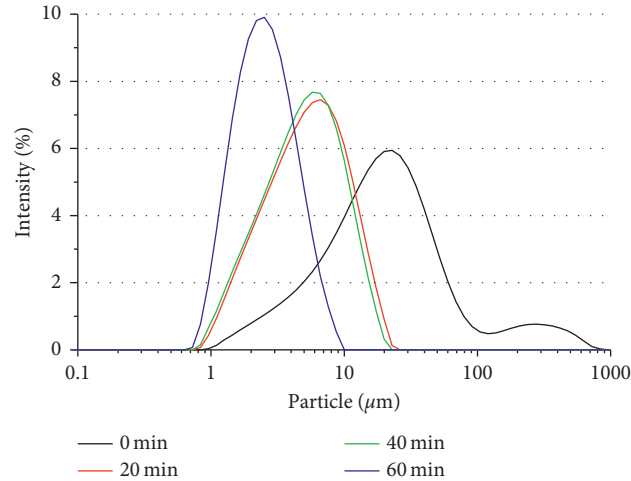


FIGURE 1: Different particle size distributions of slag particles at different wet milling durations.

processes before application for wet emissions. If the dry milling process is replaced by the wet milling process, the drying process can be omitted and be applied to concrete directly.

In this paper, the feasibility of UFSS prepared by the wet ball mill process applied in concrete was investigated. The properties of concrete were tested by kinds of test methods and analysis methods.

2. Materials and Experimental Details

2.1. Materials

2.1.1. Ground-Granulated Blast-Furnace Slag (GGBFS). The GGBFS was from the Capital Iron and Steel Company in the state of Beijing (China). Specific gravity of GGBFS was 2.92. The particle size distribution and microstructure of slag slurry/powder for different wet milling durations and the original slag (0 min) are shown in Figure 1, Table 1, and Figure 2. The chemical composition and physical properties of slag are shown in Table 2. Compared with the original slag, the size range of UFSS was reduced and the morphology was smooth.

2.1.2. Cement. Cement was from Jidong Cement Co., Ltd, the state of Hebei province (China), Portland cement 42.5, and the specific surface area is $316 \text{ m}^2/\text{kg}$. The physical and mechanical properties of cements are shown in Table 2.

2.1.3. Other Materials. The fine aggregates and coarse aggregates used were natural river sand and broken stones. Maximum particle size of fine aggregates and coarse aggregates was 2.36 mm and 20 mm, respectively. Fineness modulus of fine aggregates was 2.7. Table 3 shows the properties of coarse and fine aggregates of concrete. The indicator test methods were carried out according to the Chinese national standards GB14684-2011 and GB14685-2011.

TABLE 1: The main integral distribution of slag powder at different wet grinding times.

Sample	$d(0.1)$ (μm)	$d(0.5)$ (μm)	$d(0.9)$ (μm)
0 min	4.32	18.18	70.47
20 min	1.82	5.01	11.41
40 min	1.734	4.73	10.59
60 min	1.21	2.32	4.62

2.2. Experimental Details

2.2.1. Experimental Design. The durations of grinding were 20 min (UFSS20), 40 min (UFSS40), and 60 min (UFSS60) which were used to replace Portland cement with different percentages, namely, 20, 35, and 50, and were designed to compare portland cement with original slag concrete (from B1 to E3, Table 4). Consulting the literature [13–16], 10–60% of slag replace cement in concrete displays good performance, and the fineness of slag can also make a difference. In this study, the specimens of compressive strength and workability were concrete, and that of microstructure tests were corresponding paste. The designations of mixtures are shown in Table 4; the concrete mix proportion is cement : water : sand : stone = 1 : 0.5 : 1.57 : 2.36. The mixture codes in Table 4 are the percentage figures, which indicated the weight percentage between different raw materials.

2.2.2. Wet Ball Milling Details. The ball crusher is YXQM-2L, the grinding speed is 400 r/min, the ratio of water to solid is 0.5, the ratio of ball to materials is 4, and the milling media are $\Phi 8$ mm agate ball and $\Phi 3$ mm zirconia ball.

2.2.3. Specimen Preparation. GGBFS and water were mixed and ground. Firstly, different UFSS were obtained through controlled grinding duration based on the milling curve. Then, the UFSS was mixed with the remaining water during the preparation of the specimen, and the other conventional steps were carried out according to the Chinese national standard GB/T 50081-2002.

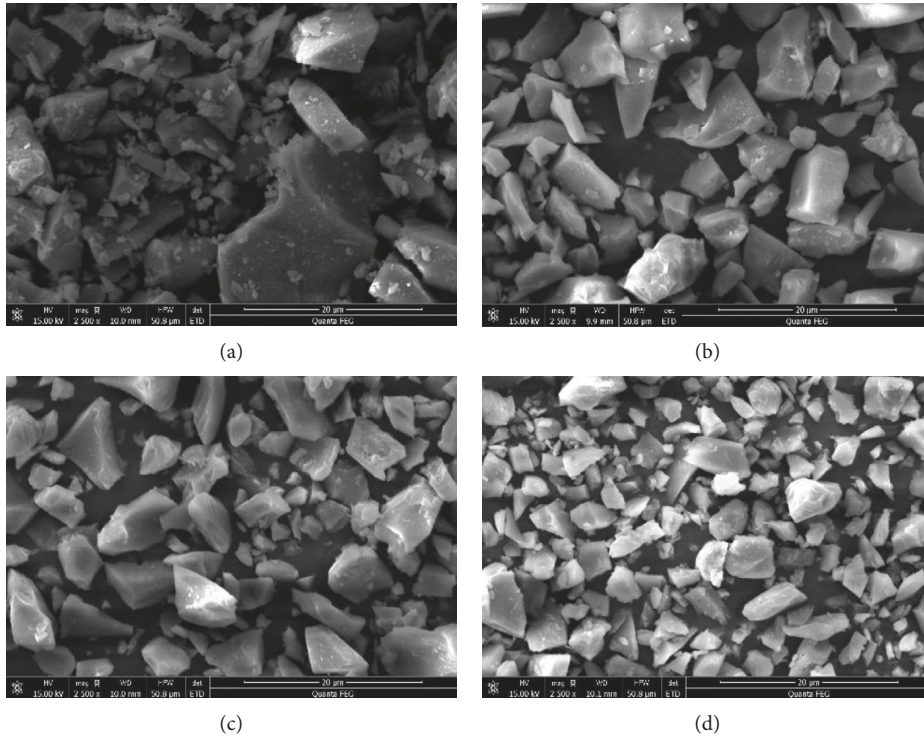


FIGURE 2: SEM images of slag powder at different wet grinding times: (a) raw slag and wet grinding for (b) 20 min, (c) 40 min, and (d) 60 min.

TABLE 2: Chemical composition of GGBFS and cement.

	Oxide composition of GGBFS (wt.%)	Oxide composition of cement (wt.%)
SiO ₂	33.50	23.03
Al ₂ O ₃	12.52	5.11
Fe ₂ O ₃	1.10	3.34
CaO	37.90	63.33
MgO	9.29	2.06
SO ₃	2.51	2.33

TABLE 3: The properties index of coarse and fine aggregates of concrete.

	Grading	Mud content (%)	Apparent density (kg/m ³)	Bulk density (kg/m ³)
Coarse	Continuous	0.4	2773	1458
Sand	II level	1.6	2659	1463

2.3. Testing Methods

2.3.1. Flowability. The flowability tests of the fresh mixed concrete were performed in conformity with the Chinese national standard GB/T 2419-2005.

2.3.2. Compressive Strength. The compressive strength tests were performed in conformity with the Chinese national standard GB/T 17671-2005, and the ages were 3 days, 7 days, 28 days, and 90 days.

2.3.3. Scanning Electron Microscopy (SEM). The microstructure of specimens of 28 days was tested by scanning electron microscopy (FEI Quanta 450FEG), with the magnification of $\times 2000$ and $\times 10000$.

2.3.4. X-Ray Diffraction (XRD). The model of laboratory X-ray diffraction used was D/MAX-RB (RIGAKU Corporation, Japan). The test angle range was $5\text{--}70^\circ$, and the test error was controlled within 0.02° ($\Delta 2\theta \leq \pm 0.02^\circ$). The age of specimens was 28 days.

2.3.5. Mercury Intrusion Porosimetry (MIP). The microporous structure of specimens at 28 days was tested by mercury intrusion porosimetry complying ISO 15901-1:2005. The porosity, median pore diameter of area, and the average pore diameter of hydration production were analyzed using Demo windows 9400 series software.

3. Results and Discussion

3.1. Workability. The workability is the ease of working with a freshly mixed concrete in the stages of handing, placing, compacting, and finishing. Slump is always regarded as an indicator of the workability of concrete [14]. To explore the feasibility of UFSS replace cement in concrete, the slump was tested and is depicted in Figure 3.

The content and grinding duration of UFSS reduced slump. Mixing E3 with 50% UFSS60 showed a slump value of 169 mm as compared to 180 mm and 174 mm showed by mixtures E1 and E2 which had 20% and 35% UFSS60.

TABLE 4: Designations of mixtures in this research.

Number		GGBFS		Cement (wt.%)	Sand (wt.%)	Coarse (wt.%)	Water (wt.%)
		Content (wt.%)	Milling duration (min)				
A	A1	0	—	100	157	236	50
B	B1	20	0	80	157	236	50
	B2	35	0	65	157	236	50
	B3	50	0	50	157	236	50
C	C1	20	20	80	157	236	50
	C2	35	20	65	157	236	50
	C3	50	20	50	157	236	50
D	D1	20	40	80	157	236	50
	D2	35	40	65	157	236	50
	D3	50	40	50	157	236	50
E	E1	20	60	80	157	236	50
	E2	35	60	65	157	236	50
	E3	50	60	50	157	236	50

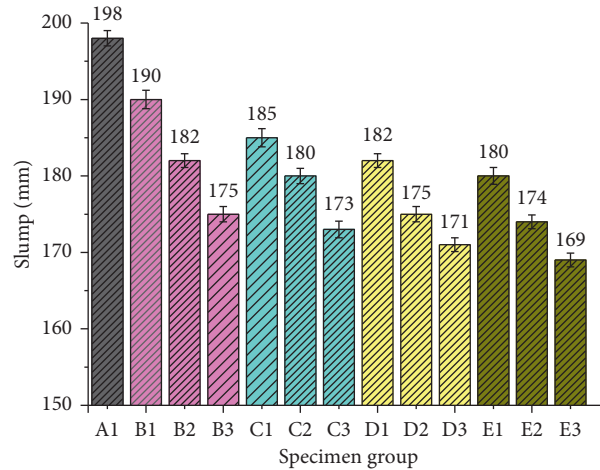


FIGURE 3: Slump of mixture with different contents and milling durations.

Similarly discipline was observed in series A, B, C, and D. The increase of content of slag decreased the fluidity, which confirmed the trend obtained by Deb et al. [14]. Under the condition of same dosage of slag, take 35% as an example, the slump of C2, D2, and E2 were reduced by 5.3%, 7.9%, and 8.4%, respectively, compared to B2. Similarly discipline was observed in 20% and 50% series.

The slump was decreased slightly with the increase of content and milling duration extended for slag. The results of this part were similar to the results of literatures [17, 18]. The reasons for that were that the increases of surface of slag powder led to increased water demand. What is more, the slag was contacted with the aqueous medium directly, and the vitreous network of slag particles is more easily to be dissolved in the process of wet ball milling. The surface of the slag particles becomes rough, leading to poor workability. This may be a further reason for the above results.

3.2. Compressive Strength. The results of compressive strength tests of specimens at different ages are depicted in

Figure 4. UFSS could accelerate the development of compressive strength at the early age of concrete. For E3 with 50% of UFSS60, the 3-day strength reached 60.1% of that of 28 days, while the values of B3, C3 and, D3 were found to be 48.1%, 56%, and 58.7%, respectively. For 50%, the ratios of 7 and 28 days strength of original slag, UFSS20, UFSS40, and UFSS60 were found to be 63.7%, 65.7%, 69.3%, and 74.2%, respectively.

The above results confirmed the trend obtained in dry ground slag by Yan Shi and Arash Aghaeipour [19, 20]. The reasons for the above results may be the disparity of activity and particle size of slag. The average diameter ($d(0.5)$) of UFSS20, UFSS40, and UFSS60 was $5.01\ \mu\text{m}$, $4.73\ \mu\text{m}$, and $2.32\ \mu\text{m}$, respectively, while that of original slag was $18.18\ \mu\text{m}$. The compactness of concrete was improved, and the large pores were reduced effectively (specification in Section 3.3 specifically). Sharmila and Dhinakaran [21] studied the compressive strength of commercially available ultrafine slag applied to the concrete. They found that the performance of concrete was improved. The study [22] showed that the activity of slag was lower than that of cement and failed to exhibit considerable reaction in the early age.

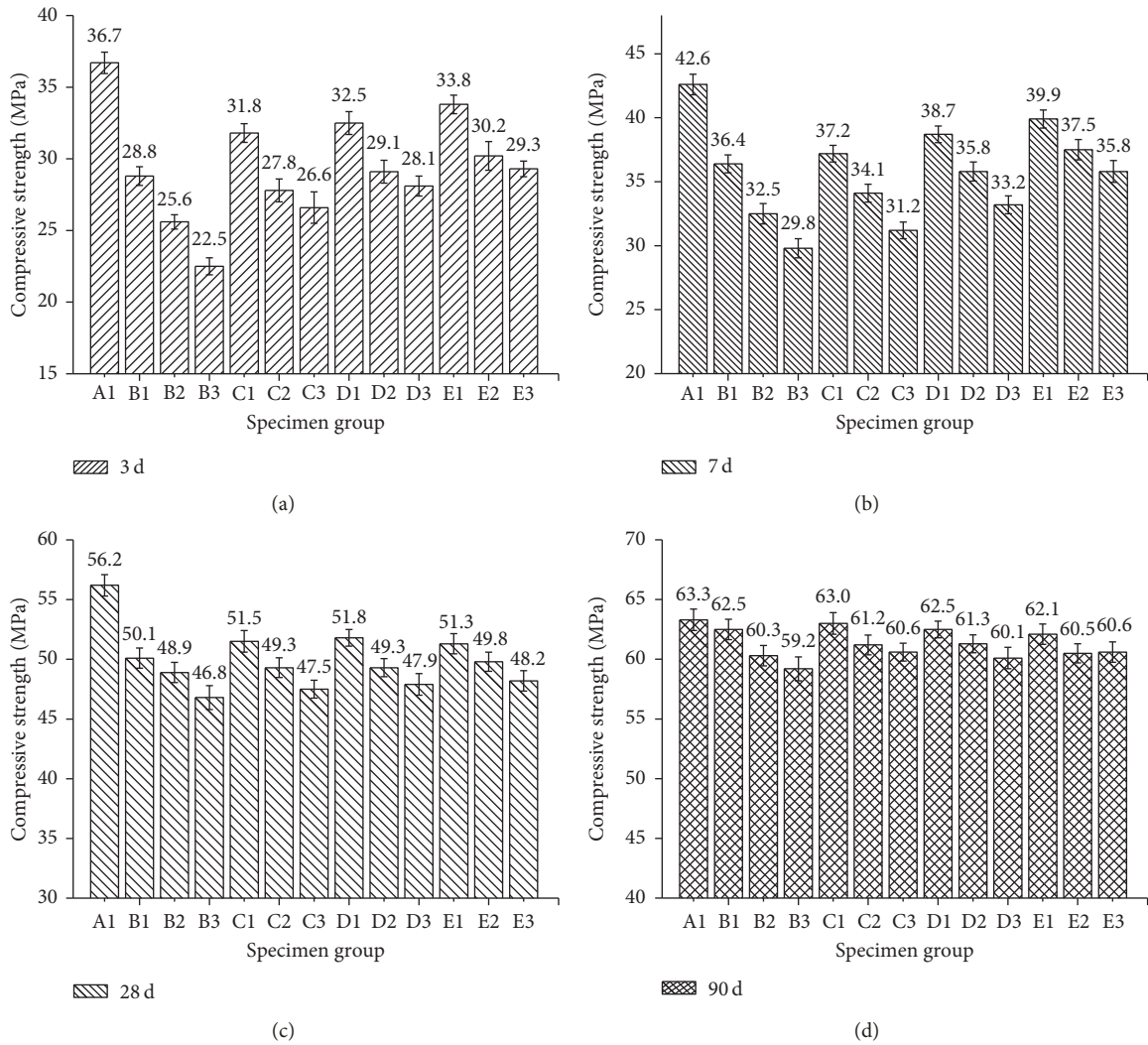


FIGURE 4: Compressive strength of specimens at different ages.

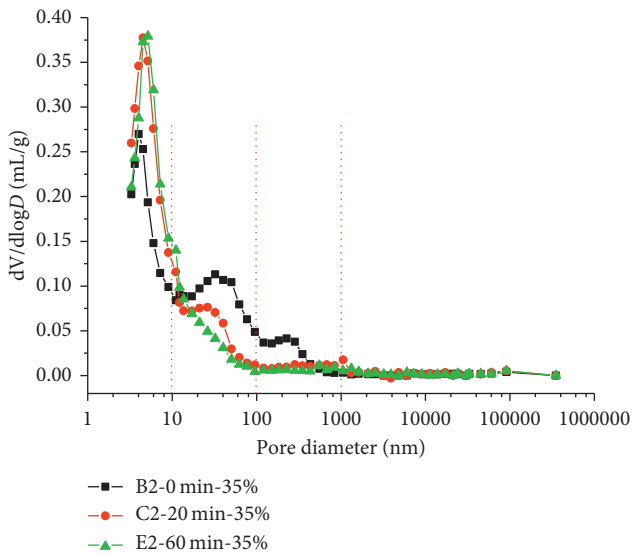


FIGURE 5: Pore size distribution curves of specimens with 35% of UFSS at 28 days.

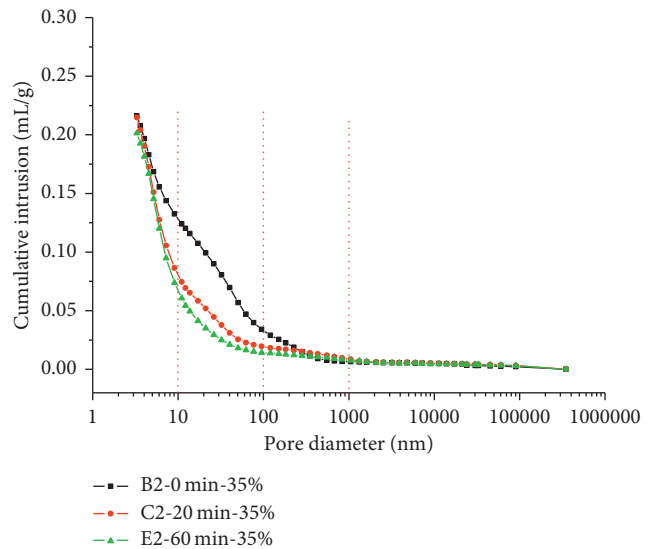


FIGURE 6: Cumulative pore volumes of specimens with 35% of slag cured for 28 days.

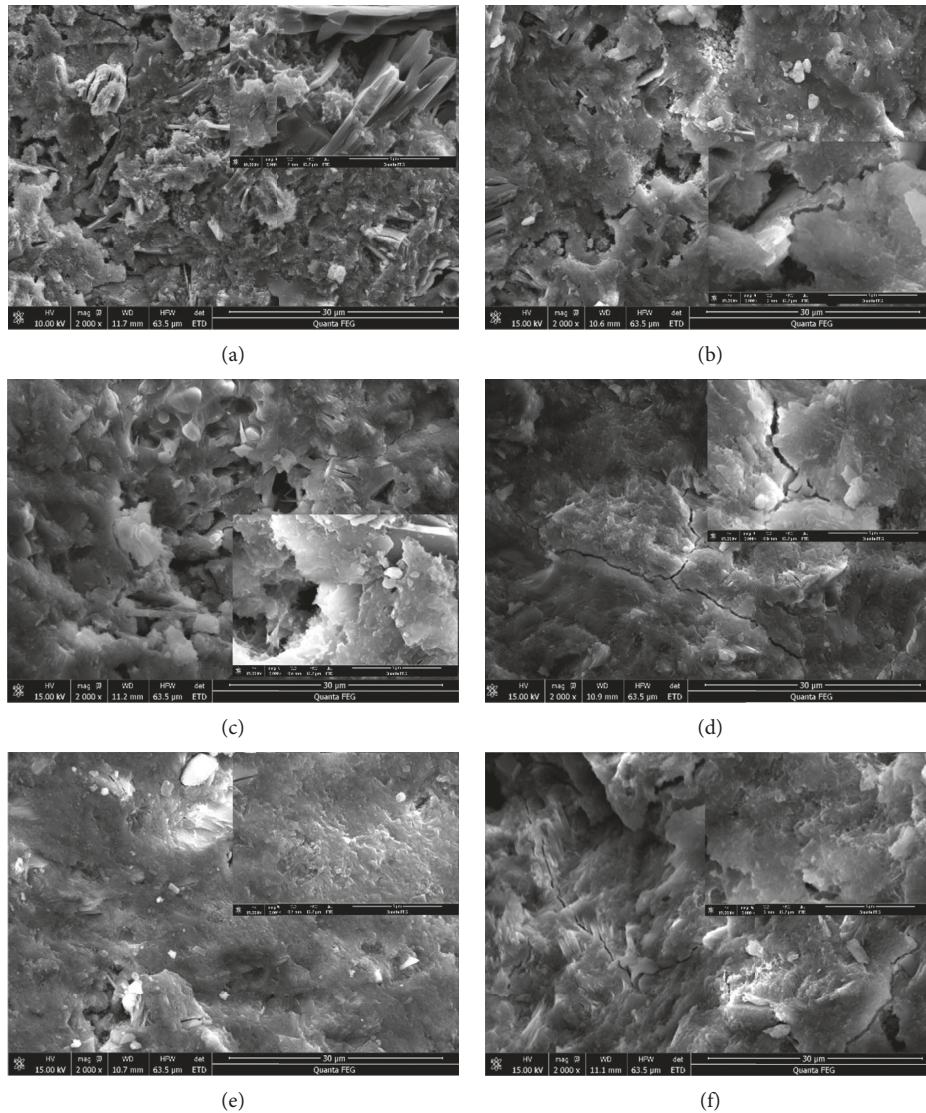


FIGURE 7: SEM images of specimens cured for 28 days: (a) B2-0 min-35%, (b) C2-20 min-35%, (c) D1-40 min-20%, (d) D2-40 min-35%, (e) D3-40 min-50%, and (f) E2-60 min-35%.

The activity of slag disposed by the milling process was improved, which was beneficial for the improvement of compressive strength especially in early ages.

The results of compressive strength at ages 28 days and 90 days showed that the compressive strength of specimens decreased with the increase of slag content and increased with the duration of grinding extend. The gaps of compressive strength of specimens become smaller with the extension of age. Sharmila and Dhinakaran [23] found that the compressive strength of concrete was reduced when the content of ultrafine slag exceeded 15%. The aggregation of fine particles leads to a higher porosity. However, this phenomenon was not observed with slag of 50% in this study. The wet ball mill was carried out in aqueous media, the surface of the particles formed hydrated films under the effect of aqueous media, and the surface energy of particles was relatively lower to the dry ball mill. What is more, the

UFSS was mixed with water first and then mixed together with other raw materials; the particles get a good dispersion in the concrete.

3.3. Pore Structure. The results of pore size distribution (PSD) of B2, C2, and E2 at 28 days are shown in Figure 5. UFSS refined the pores and created a distribution peak for the pore range within 100 nm, and the trend was clearly observed in the specimens with UFSS60. Three characteristic ranges of pore sizes were divided: <10 nm (Part I), 10 nm–100 nm (Part II), and >100 nm (Part III), with various peaks in each range, which represent small pores, middle capillary pores, and larger capillary pores [24].

For specimens incorporating 35% of UFSS, the pattern of PSD curves was significantly different for different grinding durations. B2 samples (original slag, 35%) present triplet

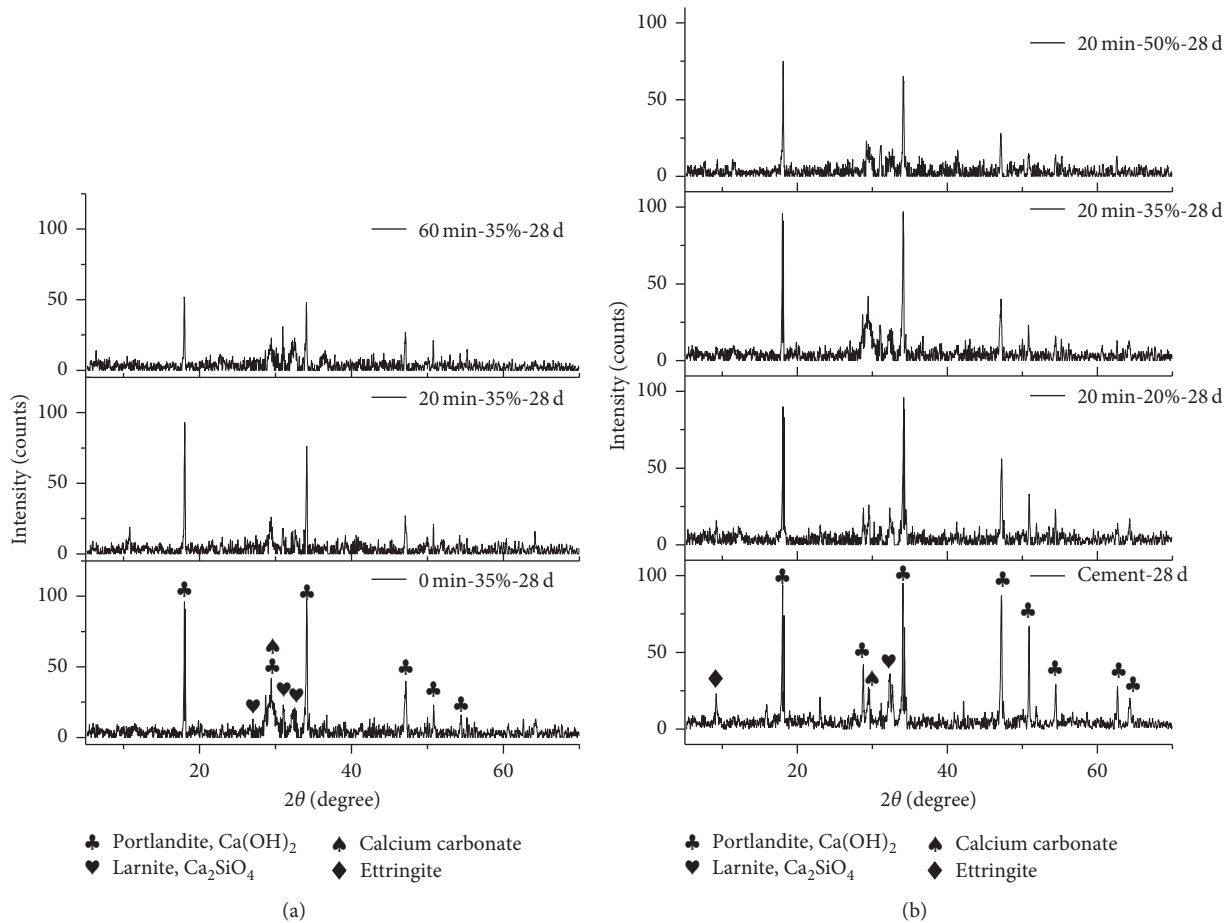


FIGURE 8: XRD of the specimens cured for 28 days.

peak characteristics in Part I, Part II, and III. The pores consisted of small pores, middle capillary pores, and larger capillary pores. C2 samples (UFSS20, 35%) present dual peak characteristics in Part I and Part II. The pores were refined and mainly consisted of small pores and middle capillary pores. E2 samples (UFSS20, 35%) present single peak characteristics in Part I, which mainly consists of small pores.

For the range of Part I, the formation of small pores was mainly the hydration of cementitious materials [24, 25]. The hydration extent of B2 was limited compared to the other two groups. The values of C2 and E2 were close, indicating that the extents of hydration reaction were similar with an age of 28 days. For the range of Part II, the pores >10 nm were formed by the filling effect of particles in concrete [26]. The peak of the PSD curve of B2 was obvious; the compactness of hardened body was poor relatively. The peak of the PSD curve of C2 exits and is weaker than B2, indicating that UFSS20 could improve the compactness of concrete compared to original slag. E2 showed a smooth curve in this part, indicating that the compactness of concrete could be improved obviously. For the range of Part III, only the curves of B2 exit a peak. UFSS obtained from wet milling could improve the compactness of concrete effectively.

Figure 6 shows the cumulative pore volumes of the specimens corresponding to Figure 5. As the particle size of slag

reduces, the pore volume decreased. The porosities of B2, C2, and E2 were 24.7986%, 24.0260%, and 23.7765%, respectively. The porosities decreased with the reduction of sizes of particles. The slag slurry reduced the distribution of larger pores and optimized the porosity distribution. The compactness and compressive strength of concrete were optimized.

3.4. Microstructure Tests. Figure 7 shows the SEM images of specimens incorporating UFSS at 28 days. The larger capillary pores were easily observed in B2. From the images of D1, D2, and D3, the compactness of specimens was improved with the increasing of slag content. Ultrafine slag particles played an important role in the compactness performance of hardened body. The compactness of pates was improved with the grind duration extending, which was consistent with the results of MIP tests. This further explained the increase of compressive strength of concrete with ultrafine slag.

The cement particles were wrapped by slag particles, causing delay of the reaction process for cement particles, and the hydrated products of cement particles were not easily observed. However, the activity of slag particles was lower than that of cement particles even through the milling process. This was why the compressive strength decreased with the increased content of slag, even if the porosity was improved.

3.5. *X-Ray Diffraction Analysis.* XRD analysis was carried out to examine the influences of the content and fineness of slag on hydration and phase. XRD images are shown in Figure 8. From XRD analysis, mineral phases of portlandite, calcium carbonate, larnite, and ettringite were found.

In the cement paste blended with slag, three structure reactions were involved: cement hydration, the pozzolanic reaction of slag, and hydration reaction of slag [27, 28]. However, slag exhibits a pozzolanic reaction in the presence of calcium hydroxide ($\text{Ca}(\text{OH})_2$) formed upon cement hydration [20]. The extent of slag involved in the reaction could be reflected by the amount of calcium hydroxide under same content conditions. It could be seen from the XRD images (Figure 8(a)) that the content of calcium hydroxide decreased with the decrease of particle size. The results illustrated that the activity slag treated through wet milling was increased, which accounted for the increase of compressive strength. With different slag dosages, the test results of various contents of slag (Figure 8(b)) complied with the above regularity: the amount of calcium hydroxide reduced with the increase in content.

4. Conclusion

This study investigated the influences of ultrafine slag slurry (UFSS) prepared by the wet ball mill on the properties of cement and concrete. The results obtained were summarized as follows:

- (i) Wet ball mill could improve the size distribution of slag particles effectively. The slag decreased the slump of concrete slightly.
- (ii) Use of UFSS as a substitute to cement improved the compressive strength of concrete especially at early ages.
- (iii) UFSS optimized the pore size distribution of the plaster. The amount of large pores (10–100 nm) were decreased notably and created distribution in the range of small pores (<10 nm).

Conflicts of Interest

The authors declare that there are no conflicts of interest regarding the publication of this article.

Acknowledgments

The authors gratefully acknowledge the support of the National Key Research and Development Plan (no. 2017YFB0310003) and the Science and Technology Support Program of Hubei Province (no. 2017ACA178) for funding this project.

References

- [1] G. Tesema and E. Worrell, “Energy efficiency improvement potentials for the cement industry in Ethiopia,” *Energy*, vol. 93, no. 2, pp. 2042–2052, 2015.
- [2] J. Li, P. Tharakan, D. Macdonald, and X. Liang, “Technological, economic and financial prospects of carbon dioxide capture in the cement industry,” *Energy Policy*, vol. 61, no. 10, pp. 1377–1387, 2013.
- [3] C. L. H. Wang and C. Y. Lin, “Strength development of blended blast furnace slag cement mortars,” *Journal of the Chinese Institute of Engineers*, vol. 9, no. 3, pp. 233–239, 1986.
- [4] M. C. G. Juenger and R. Siddique, “Recent advances in understanding the role of supplementary cementitious materials in concrete,” *Cement and Concrete Research*, vol. 78, pp. 71–80, 2015.
- [5] A. A. Ramezani-pour, “Effect of curing on the compressive strength, resistance to chloride-ion penetration and porosity of concretes incorporating slag, fly ash or silica fume,” *Cement and Concrete Composites*, vol. 17, no. 2, pp. 125–133, 1995.
- [6] M. Mahoutian, Y. Shao, A. Mucci, and B. Fournier, “Carbonation and hydration behavior of EAF and BOF steel slag binders,” *Materials and Structures*, vol. 48, no. 9, pp. 3075–3085, 2015.
- [7] M. Iqbal Khan, G. Fares, and S. Mourad, “Optimized fresh and hardened properties of strain hardening cementitious composites: effect of mineral admixtures, cementitious composition, size, and type of aggregates,” *Journal of Materials in Civil Engineering*, vol. 29, no. 10, p. 04017178, 2017.
- [8] F. Puertas and A. Fernández-Jiménez, “Mineralogical and microstructural characterization of alkali-activated fly ash/slag pastes,” *Cement and Concrete Composites*, vol. 25, no. 3, pp. 287–292, 2003.
- [9] S. Kumar, R. Kumar, A. Bandopadhyay et al., “Mechanical activation of granulated blast furnace slag and its effect on the properties and structure of portland slag cement,” *Cement and Concrete Composites*, vol. 30, no. 8, pp. 679–685, 2008.
- [10] S. C. Pal, A. Mukherjee, and S. R. Pathak, “Investigation of hydraulic activity of ground granulated blast furnace slag in concrete,” *Cement and Concrete Research*, vol. 33, no. 9, pp. 1481–1486, 2003.
- [11] J. Zhao, D. Wang, and P. Yana, “Particle characteristics and hydration activity of ground granulated blast furnace slag powder containing industrial crude glycerol-based grinding aids,” *Construction and Building Materials*, vol. 104, pp. 134–141, 2016.
- [12] H. Goudarzi and S. Baghshahi, “PZT ceramics prepared through a combined method of B-site precursor and wet mechanically activated calcinate in a planetary ball mill,” *Ceramics International*, vol. 43, no. 4, pp. 3873–3878, 2017.
- [13] A. Nazari, M. H. Rafeipour, and S. Riahi, “The effects of CuO nanoparticles on properties of self compacting concrete with GGBFS as binder,” *Materials Research*, vol. 14, no. 3, pp. 307–316, 2011.
- [14] P. S. Deb, P. Nath, and P. K. Sarker, “The effects of ground granulated blast-furnace slag blending with fly ash and activator content on the workability and strength properties of geopolymer concrete cured at ambient temperature,” *Materials and Design*, vol. 62, pp. 32–39, 2014.
- [15] J. Qiu, H. S. Tan, and E.-H. Yang, “Coupled effects of crack width, slag content, and conditioning alkalinity on autogenous healing of engineered cementitious composites,” *Cement and Concrete Composites*, vol. 73, pp. 203–212, 2016.
- [16] A. Allahverdi and M. Mahinroosta, “Mechanical activation of chemically activated high phosphorous slag content cement,” *Powder Technology*, vol. 245, pp. 182–188, 2013.
- [17] Y. Tang, X. Zuo, S. He, O. Ayinde, and G. Yin, “Influence of slag content and water-binder ratio on leaching behavior of cement pastes,” *Construction and Building Materials*, vol. 129, pp. 61–69, 2016.

- [18] P. Nath and P. K. Sarke, "Effect of GGBFS on setting, workability and early strength properties of fly ash geopolymer concrete cured in ambient condition," *Construction and Building Material*, vol. 66, pp. 163–171, 2016.
- [19] A. Aghaeipour and M. Madhkhan, "Effect of ground granulated blast furnace slag (GGBFS) on RCCP durability," *Construction and Building Materials*, vol. 141, pp. 533–541, 2017.
- [20] Y. Shi, H. Chen, J. Wang, and Q. Feng, "Preliminary investigation on the pozzolanic activity of superfine steel slag," *Construction and Building Materials*, vol. 82, pp. 227–234, 2015.
- [21] P. Sharmila and G. Dhinakaran, "Compressive strength, porosity and sorptivity of ultra fine slag based high strength concrete," *Construction and Building Materials*, vol. 120, pp. 48–53, 2016.
- [22] A. Karimpour, "Effect of time span between mixing and compacting on roller compacted concrete (RCC) containing ground granulated blast furnace slag (GGBFS)," *Construction and Building Materials*, vol. 24, no. 11, pp. 2079–2083, 2010.
- [23] P. Sharmila and G. Dhinakaran, "Strength and durability of ultra fine slag based high strength concrete," *Structural Engineering and Mechanics*, vol. 55, no. 3, pp. 675–686, 2015.
- [24] K. Li, Q. Zeng, M. Luo, and X. Pang, "Effect of self-desiccation on the pore structure of paste and mortar incorporating 70% GGBS," *Construction and Building Materials*, vol. 51, pp. 329–337, 2014.
- [25] Q. Zeng, K. Li, T. Fen-Chong, and P. Dangla, "Pore structure characterization of cement pastes blended with high-volume fly ash," *Cement and Concrete Research*, vol. 42, no. 1, pp. 194–204, 2012.
- [26] Y. C. Choi, J. Kim, and S. Choi, "Mercury intrusion porosimetry characterization of micropore structures of high-strength cement pastes incorporating high volume ground granulated blast-furnace slag," *Construction and Building Materials*, vol. 137, pp. 96–103, 2017.
- [27] X. Feng, E. J. Garboczi, D. P. Bentz, P. E. Stutzman, and T. O. Mason, "Estimation of the degree of hydration of blended cement pastes by a scanning electron microscope point-counting procedure," *Cement and Concrete Research*, vol. 34, no. 10, pp. 1787–1793, 2004.
- [28] Y. C. Ding, T. W. Cheng, P. C. Liu, and W. H. Lee, "Study on the treatment of BOF slag to replace fine aggregate in concrete," *Construction and Building Materials*, vol. 146, pp. 644–651, 2017.

